Conf-9110313--5
CONF-9110313--5
DE92 007240

RESONANT TRANSFER EXCITATION : INTERFERENCE EFFECTS

S.M. Shafroth*, M. Benhenni*+, J.K. Swenson♦♠, M. Schulz♦✪, J.P. Giese♦△, H. Schone♦△, C.R. Vane♦, P.F. Dittner♦, and S. Datz♦

*Department of Physics and Astronomy, University of North Carolina at Chapel, Chapel Hill, NC 27599-3255, USA; +Universite Paul Sabatier, Laboratoire de Decharges dans les Gaz, Centre de Physique Atomique, 31062 Toulouse Cedex, France; ♠L421, Lawrence Livermore National Laboratory, Livermore, CA 94550, USA; ✪University of Missouri, Rolla, Department of Physics, Rolla, MO 65401, USA; △Department of Physics, Kansas State University, Manhattan, KS 66506, USA; ♦Physics Division, Oak Ridge National Laboratory, Oak Ridge, TN 37831, USA

INTRODUCTION

Interference effects in RTE (Resonant Transfer Excitation) can be studied for low Z projectiles via Auger electrons emitted from highly ionized fast moving projectile ions following collisions with low Z targets[1-18]. RTE in ion-atom collisions is closely related to dielectronic recombination[1]. In the latter case which is of practical interest to the fusion power program an electron with the proper velocity incident on a highly charged ion is resonantly captured and simultaneously interacts with an inner shell electron to excite it, thus forming a doubly excited state which may decay predominantly by x-ray emission for higher Z ions or by Auger electron decay for lower Z ions. The resonant velocity is that of the Auger electron emitted by the ion in the doubly excited state In RTE the electrons to be captured are in low Z atomic (typically He) or Molecular (typically H_2) targets and the ions are produced by accelerators in highly charged states with the appropriate resonant velocity. The resonance is much broadened by the velocity distribution of the target electrons. Thus the resonance width as a function of projectile energy is determined by folding the Compton profile of the target electrons with the dielectronic recombination cross sections. This results in a formula valid when the impulse approximation obtains:

$$\sigma_{RTE} = (M/2E)^{1/2}\Delta\varepsilon\bar{\sigma}_{RC}\Sigma J_i(p'_{iz})$$

where M and E are the projectile mass and energy respectively, $\Delta\varepsilon$ is the width of an energy bin used for averaging, σ_{RC} is the cross section for radiationless capture, $\Sigma J_i(p'_{iz})$ sums over the Compton profiles for all target electrons and $p'_{iz} = (\varepsilon_r - Em/M)(M/2E)^{1/2}$ and ε_r is the DR resonance energy[1].

There are at least two other collision processes which can lead to the same intermediate and final states, thus leading to interference. The best known is NTE (Nonresonant Transfer Excitation), an uncorrelated process where the target nucleus excites an inner electron of the projectile ion and a target electron is captured. This cross section is larger at low projectile energies and falls off slowly with increasing projectile energy. These two processes are best illustrated in data from Swenson et. al.[8]. Fig. 1 taken from (8) shows the zero degree spectra for the O^{5+} on He collision system at a variety of projectile energies. The states of interest are the $(1s2s2p^2)^3D$ and $(1s2s2p^2)^1D$ states , which decay to the $(1s^2)^2S$ ground state giving rise to $\ell=2$ Auger electrons of 449 and

455eV. The cross section vs ion energy for these transitions are shown in Fig 2 from (8). Fig 2 also shows normalized theoretical curves deduced assuming that these states are formed through RTE and NTE (at the lower projectile energies) and it can be seen that the agreement with theory is quite good.

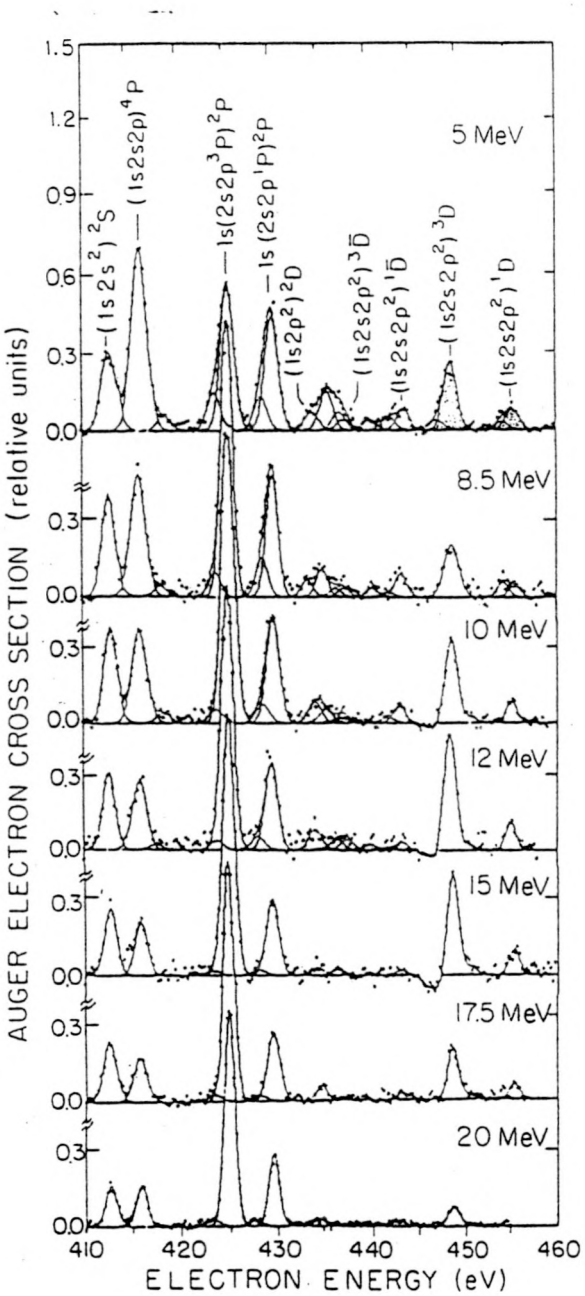

FIG. 1. High-resolution Auger-electron spectra for 0^{5+} + He for various incident ion energies. The $(1s2s2p^2)^3D$ and ^1D states refer to decay to the ionic ground state $(1s^22s)^2S$, whereas the $(1s2s2p^2)^3\overline{D}$ and $^1\overline{D}$ states refer to decay to the $(1s^22p)^2P$ final state.

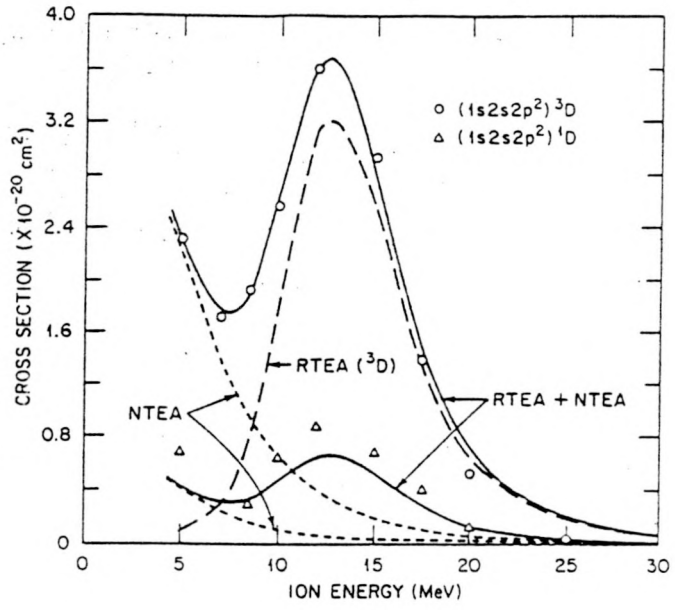

FIG. 2. Cross sections for Auger decay of the $(1s2s2p^2)^3D$ and the $(1s2s2p^2)^1D$ states to the $(1s^22s)^2S$ ground state following collisions of O^{5+} + He. The upper solid curve is an impulse-approximation-model calculation for RTE followed by Auger decay, for the ^3D state (dashed curve), superimposed on an underlying NTE-Auger background (dotted curve). The lower solid curve is the corresponding calculation for the ^1D state.

More recently Bhalla[18] worked out the theory for the effect of interference between RTE and binary encounter collisions (BE) on the Auger electron angular distributions. In this case interference was studied between an electron ejected from the target following a collision with the projectile ion (treated as a structureless charged particle) , and an Auger electron arising from decay of a doubly excited state formed via RTE. These two processes lead to the same final state and therefore can interfere. This has been known for sometime because one observes a Fano dip on the low energy side of the RTE transitions (Fig 1, 15 MeV spectrum).

A weaker effect and more speculative is Two Electron Transfer Excitation[17] (2ETE). Here one target electron excites the projectile 1s electron to the 2p shell for example and the other target electron is captured to an excited state of the projectile. This effect becomes more important at projectile energies higher than the energy where the RTE cross section has its maximum value. The electron - electron interaction has been beautifully demonstrated by Zouros et al.[19]. Finally, there might be interference with shakeup (Y. Hahn this conference). This paper will present angular distribution measurements of Auger lines so that the effects of interference between these various processes can be studied.

EXPERIMENT

THE ORNL EN tandem Van der Graaff provided up to μA beams of O^{5+} ions at energies of 6, 8, and 13 MeV where Auger electron angular distribution measurements were made. The electrons were detected with a two stage refocusing 30° parallel plate analyzer with an 8x50 mm^2 microchannel plate equiped with a resistive anode encoder in

the focal plane. Doppler broadenings caused by the variation of the observation angle, $d\Theta_L = +/- 0.4^o$ permitted by the spectrometer entrance slit width become more severe as the observation angle increases. They are eliminated to first order through refocusing of the electrons emitted from the fast moving projectiles on the detector, which is remotely positioned to the new focal position as required by the electron energy, the ion beam energy and the observation angle. The spectrometer was designed and made operational by J.K. Swenson[20]. The measurements reported here were done with 10 mT of He in the differentially pumped gas cell. Single collision conditions were ensured by studying the Auger electron yield vs pressure.

SPECTRA

Electron spectra obtained at six lab angles for 6 MeV O^{5+} projectile ions are shown in Fig 3. At each angle a polynomial fit background was subtracted from the lab spectrum. This background arises from binary encounter electrons giving rise to a broad peak which varies slowly with electron energy as well as spurious electrons due to recoil ions which enter the spectrometer when positive deceleration voltages are present. Next an efficiency correction for the location of the Auger lines on the channel plate is applied[21]. Following this the spectra were transformed from lab to projectile frame. As has been said above, the transition of primary interest is the $(1s2s2p^2)^3D$ to ground state, but less good data has been obtained for the $(1s2s2p^2)^1D$ to ground state and is reported in (21) as is data for H_2 target gas. In order to obtain Angular distributions for the $\ell = 2$ $^3D \rightarrow {}^2S$ transition, its differential cross section was normalized to the $\ell = 0$ ground state decay of a three electron excited state $(1s2s^2)^2S$ at 412 eV. which are assumed to be isotropic This serves to eliminate errors arising from beam current integration, target length, solid angle and gas pressure drifts.

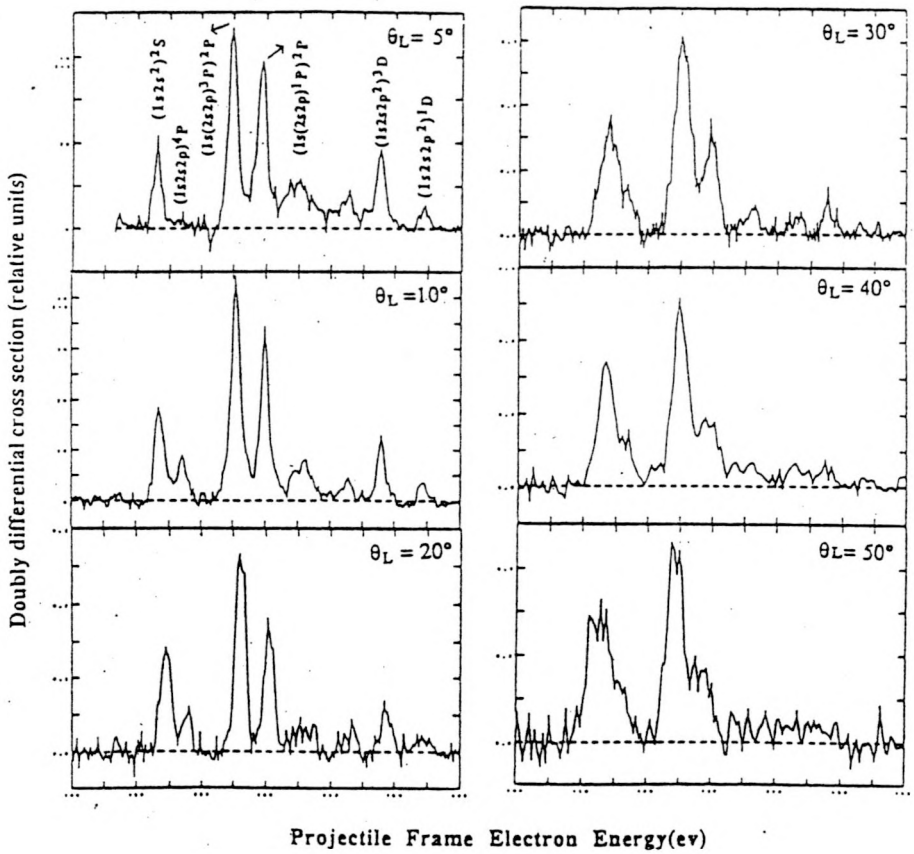

FIG. 3 Auger electron spectra in the projectile frame at various lab angles θ_L obtained following O^{5+} + He collisions at 6 MeV O^{5+} projectile energy.

From Fig. 3 it can be seen that that the resolution deteriorates significantly as Lab angle increases. Also the cross section for production of ^3D decreases with increasing lab angle. The projectile angle is slightly less than twice the lab angle at 6 MeV, whereas at 13 MeV where RTE reaches its maximum. the projectile angle is twice the lab angle.

ANGULAR ANGULAR DISTRIBUTIONS

1) RTE-BE Interference

In order to study RTE - BE interference effects relative angular distributions were measured at 13 MeV where the RTE transition falls at the same energy as the maximum of the binary encounter peak[21]. In Fig 4 the ratio $[d\sigma/d\Omega(^3D)]/[d\sigma/d\Omega(^2S)]$ is plotted as circles versus laboratory angle. The error bars in the data result from background subtraction and counting statistics. The solid line represented in Fig. 4 is the recent calculation by Bhalla[18] for our collision system O^{5+} + He. It was obtained by use of the

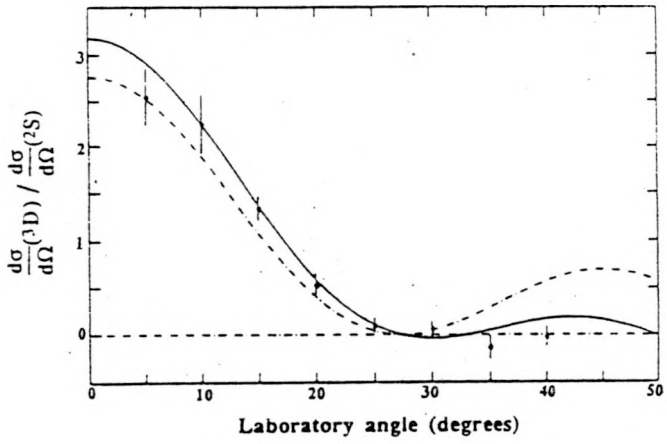

FIG. 4. The circles are the experimental ratios $(d\sigma/d\Omega)(^3D)/(d\sigma/d\Omega)(^2S)$ vs laboratory angle for 13-MeV projectile O^{5+} on He. The solid line represents Bhalla's theory[18], normalized to experiment at $\theta_L = 10°$. The dashed line is the resonance contribution $C_R(E_R,\theta_L)$ to the RTEA differential cross section, excluding the interference between RTEA and BE.

RTEA angular-dependent impulse approximation[18] and given by

$$\left[\frac{d\sigma}{d\Omega}(^3D)\right]_{RTEA} = C_R(E_R,\theta_L) + C_1(E_R,\theta_L), \qquad (1)$$

where $[d\sigma/d\Omega(^3D)]_{RTEA}$ is the difference between the total differential cross section for electron emission and the binary-encounter differential cross section. The term C_R represents the contribution of the Auger angular distribution of the RTEA resonance and C_1 is the contribution from the interference between RTEA and the elastic binary-encounter channel. E_R and θ_L are the resonance energy and the laboratory emission angle, respectively. The dashed curve in Fig. 4 is a plot of the resonance term C_R alone, which corresponds to a pure spherical harmonic $|Y_{20}|^2$. Thus the observed anisotropy of the RTEA angular distribution results from the fact that the ^3D state is exclusively populated with the magnetic substate $m_l = 0$. This is expected since in RTE, the exchange of angular momentum takes place solely between two electrons and the transferred target electron

carries no net angular momentum into the collision. Since we measured a ratio of cross sections, the theory has been scaled by a factor of 0.56 to normalize the theory to the data at 10°. By comparing the solid and the dashed curves, relatively small constructive interference between RTEA and the elastic binary-encounter channels is indicated in the forward direction, while strong destructive interference occurs when θ_L is greater than 25°.

Earlier measurements of RTEA performed at 0° emission angle show that the total RTEA cross section for the system O^{5+} + He, after very careful spectrometer efficiency determination[22] and assuming isotropy of the angular distribution, is larger by a factor of 3.5 than theory.[23] After correction for measured anisotropy of the RTEA angular distribution, the total cross section σ_t, given by $[4\pi/(2l + 1)]d\sigma/d\Omega$ ($\theta_L = 0°, m_l = 0$), becomes lower than theory by a factor of 0.7. Thus an improved agreement between experiment and theory is obtained when the measured angular distribution for the state in question is used.

In summary, we have measured the angular distribution of the $(1s2s2p^2)^3D$ Auger ground-state decay at the resonance energy of 13-MeV O^{5+}. The data show an angular distribution strongly peaked along the beam axis direction. Furthermore, at this resonance energy, the data show a small constructive interference between the RTEA and the elastic binary-encounter channels in the forward direction and strong destructive interference at laboratory angles greater than 25°. Our results are in good agreement with Bhalla's recent calculations of the RTEA angular-dependent impulse approximation.

The correction of earlier RTEA measurements for anisotropy in the angular distribution improves the agreement between the experiment and theory and gives a stringent test of the impulse approximation.

2) RTE-NTE Interference

In order to study RTE-NTE interference effects, relative angular distributions of $^3D \rightarrow {}^2S + \epsilon$ ($\ell = 2$) transitions were measured at 6 and 8 MeV in addition to that of 13 MeV. In fig. 5 the ratios $[d\sigma/d\Omega(^3D)]/[d\sigma/d\Omega(^2S)]$ are plotted versus projectile emission angle θ_p at the projectile energies 6, 8 and 13 MeV, where $d\sigma/d\Omega(^3D)$ and $d\sigma/d\Omega(^2S)$ are the respective Auger ground state decay differential cross sections of the ^3D and the ^2S excited states respectively. The projectile angle θ_p was obtained from the lab emission angle θ_L by the kinematic frame transformations. The solid lines are linear least squares fits to the data represented by $W(\theta_p) = C[1+a_2P_2(\cos\theta_p)+a_4P_4(\cos\theta_p)]$ given by angular momentum theory, where $P_2(\cos\theta_p)$ and $P_4(\cos\theta_p)$ are the second and forth order Legendre polynomials respectively. Fig. 5 shows that the ^3D angular distributions are forward peaked along the beam direction, more forward peaked at the resonance energy 13 MeV where RTE populates the ^3D state predominantly[8], than at the energies 6 and 8 MeV where NTE has a significant contribution[8]. Furthermore, the ^3D angular distribution at 8 MeV projectile energy where RTE and NTE have equal magnitudes[8], is less forward peaked than the angular distribution at 13 MeV energy where RTE predominates or at 6 MeV where NTE predominates. This suggests that destructive interferences may be taking place between the RTE Auger (RTEA) and NTE Auger (NTEA) in the forward direction. This result is in agreement with previous calculations by T. Reeves[13], where a dip occurs in the ^3D energy dependence cross section after adding coherently the magnitudes for RTE and NTE. This destructive interference was also suggested by Itoh et. al.[7] to explain the positive shift of the resonance energy and the smaller width of the resonance than the predicted value by the Impulse approximation. They claimed that this departure of the peak position and width from the theory can be understood if the RTE and NTE amplitudes interfere destructively and therefore the RTE and NTE amplitudes are added coherently.

Furthermore, the magnetic substate population probabilities Q(lm) were inferred from the anisotropy coefficients as follows:

$$Q(20) = 0.2[1 + a_2 + a_4]$$
$$Q(2\pm1) = 0.2[1 + 0.5a_2 - 0.66a_4]$$
$$Q(2\pm2) = 0.2[1 - a_2 + 0.15a_4]$$

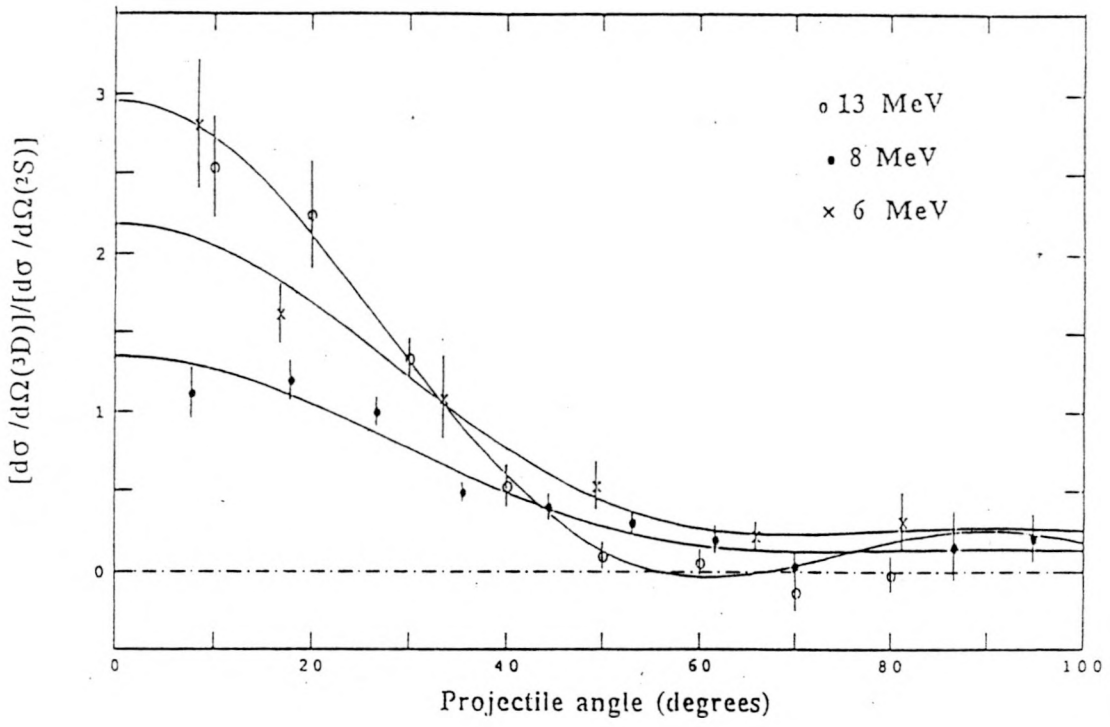

Fig. 5. Relative angular distributions of the $(1s2s2p^2)^3D$ Auger decay to ground state $(1s^22s)^2S$ at 6, 8, and 13 MeV 0^{5+} energies. The solid lines are least squares fits to the data and are given by $W(\theta_p)=C[1+a_2P_2(\cos\theta_p)+a_4P_4(\cos\theta_p)]$.

Table 1. Magnetic substate population probabilities of the $(1s2s2p^2)^3D$ formed following O^{5+} collisions with He.

E(MeV)	Target	$a_2 \pm \Delta a_2$	$a_4 \pm \Delta a_4$	$Q(20)\pm \Delta Q(20)$	$Q(2\pm1)\pm \Delta(Q2\pm1)$	$Q(2\pm2)\pm \Delta Q(2\pm2)$
13	He	3.43 ± 0.88	2.26 ± 1.18	1.33 ± 0.50	0.24 ± 0.28	-0.40 ± 0.40
8	He	1.92 ± 0.34	0.97 ± 0.25	0.79 ± 0.08	0.26 ± 0.05	-0.15 ± 0.05
6	He	1.80 ± 0.33	1.03 ± 0.37	0.77 ± 0.11	0.24 ± 0.06	-0.13 ± 0.07

Table 1 shows that the ^3D state is exclusively populated with the magnetic substate $m_\ell=0$ at the resonance energy of 13 MeV where RTE predominates in agreement with Bhalla's calculations[18]. However, at 6 and 8 MeV projectile energies where NTEA plays a significant role in populating the ^3D state, small contributions from the magnetic substates $m_l=\pm1$ are also observed. The presence of the magnetic substate $m_l=\pm1$ at these energies can be understood since the electron excitation is caused by the target nucleus therefore changing the initial angular momentum $m_l=0$ whereas, in RTE the interaction is electron electron interaction[18] of the type $1/r$ and therefore conserves the initial angular momentum $m_\ell=0$. The negative values of $Q(2\pm2)$ shown in table 1 may be attributed to contributions from close lying lines[21] which may have different angular distributions. These negative values may also be attributed to the destructive interferences betweenRTEA and NTEA which may introduce odd terms in the linear combination of Legendre polynomials. At the resonance energy, NTEA contribution can be neglected and the only interference contribution is the interference between RTEA and the binary encounter process which varies as $P_2(\cos\theta_L)$ in the angular range considered here[18]. Therefore, the sum of the resonance term and the interference term is well fitted with a linear combination of only even order Legendre polynomials. Here, the interference of RTE with 2eTE can be neglected since the threshold energy for the 1s-2p excitation is 16.3 MeV.

In summary, we have measured the angular distributions of the ^3D Auger decay to ground state in collisions of O^{5+} with He. The data show that the angular distributions are forward peaked along the beam direction, more forward peaked at the resonance energy of 13 MeV where RTE is predominant than at 6 or 8 MeV projectile energies where NTE plays a significant role in the formation of the ^3D state. Furthermore, the ^3D angular distribution at 8 MeV projectile energy where RTE and NTE have equal contribution, is less forward peaked than at 13 MeV where RTE predominates or at 6MeV where NTE predominates. This suggests that destructive interferences between RTEA and NTEA may be taking place in the forward direction in agreement with previous calculations. Moreover, the magnetic substate population probabilities have been inferred from the angular momentum coupling theory and show that the ^3D state is exclusively populated with the magnetic substate $m_l=0$ at 13 MeV. However, at 6 and 8 MeV projectile energies, where NTE is important, small contributions from the magnetic substates $m_\ell = \pm 1$ are also observed. Moreover, the negative values of $Q(2\pm2)$ off resonance, where NTE plays a significant role may be attributed to destructive interference between RTE and NTE.

ACKNOWLEDGMENTS: We acknowledge support by the U.S. Department of Energy, Office of Basic Energy Sciences, Division of Chemical Sciences, under contracts No. DE-FG05-87ER40361 with Martin Marietta Energy Systems, Inc. and the University of North Carolina Research Council.

REFERENCES

1) D. Brandt, *Phys. Rev.* **A27**, 1314 (1983).
2) D. Brandt, *Nucl. Inst. and Meth.* **214**, 93 (1983).
3) J.M. Feagin, J.S. Briggs, and T.M. Reeves, *At. Mol. Phys.* **117**, 1057 (1984) and *J. Phys.* **B17**, 1057 (1984).
4) M. Clark, D. Brandt, J.K. Swenson, and S.M. Shafroth, *Phys. Rev. Lett.* **54**, 544 (1985).
5) J.A. Tanis, E.M. Bernstein, M. Clark, W.G. Graham, R.H. McFarland, T.J. Morgan, B.M. Johnson, K.W. Jones, and M. Meron, *Phys. Rev.* **A31**, 4040 (1985).
6) P.L. Pepmiller, P. Richard, J. Newcomb, J. Hall, and T.R. Dillingham, *Phys. Rev.* **A31**, 734 (1985).
7) A. Itoh, T.J.M. Zouros, D. Schneider, U. Stettner, W. Zeitz and N. Stolterfoht, *J. Phys.* **B**: *At. Mol. Phys.* **18**, 4581 (1985).
8) J.K. Swenson, Y. Yamazaki, P.D. Miller, P.F. Dittner, P.L. Pepmiller, S. Datz, and N. Stolterfoht, *Phys. Rev. Lett.* **57**, 3042 (1986).
9) J.K. Swenson, J.M. Anthony, M. Reed, M. Benhenni, S.M. Shafroth, D.M. Peterson, and L.D. Hendrick, *Nucl. Inst. and Meth.* **B24/25**, 184 (1987).
10) J.M. Anthony, S.M. Shafroth, M. Benhenni, E.N. Strait, T.J.M. Zouros, L.D. Hendrick, and D.M. Peterson, *Journal de Physique, colloque* C9, supplement au NO 12, tome 48, 301 (1987).
11) M. Schulz, E. Justiniano, R. Schuch, P.H. Mokler, S. Reusch, *Phys. Rev. Lett.* **58**, 1734 (1987).
12) W. Fritch and C.D. Lin, *Phys. Rev. Lett.* **61**, 690 (1988).
13) T. Reeves, Electronic and Atomic collisions, Elsevier Science Publishers, Invited papers of the International Conference on the Physics of Electronic and Atomic Collisions, edited by H.B. Gilbody, W.R. Newell, F.H. Read, and A.C.H. Smith (North Holland, Amsterdam) 685 (1988).
14) M. Schulz, R. Schuch, S. Datz, E.L.B. Justiniano, P.D. Miller, and H. Schone, *Phys. Rev.* **A38**, 5454 (1988).
15. T.J.M. Zouros, D.H. Lee, J.M. Sanders, J.L. Shinpaugh, T.N. Tipping, P. Richard, and S.L. Varghese, *Nucl. Inst. and Meth., Phys. Res.* **B40/41**, 17 (1989).
16) T.J.M. Zouros, D.H. Lee, T.N. Tipping, J.M. Sanders, J.L. Shinpaugh, P. Richard, K.R. Karim, and C.P. Bhalla, *Phys. Rev.* **A40**, 6246 (1989).
17) M. Schulz, J.P. Giese, J.K. Swenson, S. Datz, P.F. Dittner, H.F. Krause, H. Schöne, C.R. Vane, M. Benhenni, and S.M. Shafroth, *Phys. Rev. Lett.* **62**, 1738 (1989).
18) C.P. Bhalla, *Phys. Rev. Lett.* **64**, 1103 (1990).
19) T.J.M. Zouros, D.H. Lee, P. Richard, *Phys. Rev. Lett.* **62**, 2261 (1989).
20) J.K. Swenson, *Nucl. Inst. and Meth.* **B10/11**, 899 (1985).
21) M. Benhenni, S.M. Shafroth, J.K. Swenson, M. Schulz, J.P. Giese, H. Schöne, C.R. Vane, P.F. Dittner and S. Datz, *Phys. Rev. Lett.* **65**, 1849 (1990) and M. Benhenni, Ph.D. thesis, University of North Carolina, Chapel Hill 1990.
22) D.H. Lee, P. Richard, T.J.M. Zouros, J.M. Sanders, J.L. Shinpaugh and H. Hidmi, *Phys. Rev.* **A41**, 4816 (1990).
23) T.J.M. Zouros, C.P. Bhalla, D.H. Lee, P. Richard, *Phys. Rev.* **A42**, 678 (1990).